Polymer Chemistry

ROYAL SOCIETY OF CHEMISTRY

PAPER

View Article Online
View Journal | View Issue

Cite this: *Polym. Chem.*, 2021, **12**, 5689

Effect of hydrophilic groups on the bioactivity of antimicrobial polymers†

Phuong Pham, Susan Oliver, Edgar H. H. Wong and Cyrille Boyer *

Antimicrobial polymers have recently been investigated as potential treatments to combat multidrug-resistant pathogens. A typical antimicrobial polymer consists of cationic groups that allow the polymers to adsorb onto negatively charged bacterial membranes and hydrophobic groups that insert into and disrupt the bilipid membrane. Recently, with the introduction of ternary polymer systems, neutral hydrophilic groups have been added to modulate hydrophobic/hydrophilic balance more easily. Although numerous studies have examined the effect of active components (cationic and hydrophobic groups) of antimicrobial polymers on their bioactivity, limited studies focus on hydrophilic groups. Therefore, in this study, we developed a series of statistical amphiphilic ternary polymers to systematically investigate the effect of hydrophilic groups on antibacterial activity and biocompatibility. The results revealed that, unlike the hydrophobic groups that directly disrupt the cell membrane, the hydrophilic groups have an indirect but important impact on bioactivity through tuning of the hydrophobic/hydrophilic balance and global hydrophobicity, leading to a change in the aqueous characteristics of the polymers. Therefore, in antimicrobial polymer design, an appropriate hydrophobic/hydrophilic balance as well as the structural features of the hydrophilic group, such as length, flexibility, and hydrophilicity of the hydrophilic chain, are key determinants that can be optimised to maximise biocompatibility without negatively impacting antibacterial effect.

Received 10th August 2021,
Accepted 16th September 2021

DOI: 10.1039/d1py01075a

rsc.li/polymers

1. Introduction

From decades of antibiotic misuse and overuse, antimicrobial resistance has become an urgent threat to global public health. Up to ten million antimicrobial resistance related deaths per annum are predicted by 2050.[1] Of particular concern, multidrug-resistant (MDR) Gram-negative bacteria are associated with critical and severe illnesses and are generally more threatening to human life.[2,3] Unfortunately, no new classes of antibiotics have been approved for specific treatment of Gram-negative bacteria in over 50 years[4] and, therefore, there is an urgent need to develop new effective Gram-negative antibacterial agents.

Host-defense antimicrobial peptides (HDPs) are produced by multicellular organisms to fight against foreign pathogens.[5] These naturally occurring cationic peptides have been proposed as promising alternatives for mitigating resistance.[6–8] HDPs usually comprise from 10 to 50 amino acids and display an amphipathic cationic nature owing to their combination of cationic, hydrophobic, and hydrophilic groups.[9] They mainly kill bacteria *via* membrane disruption. As bacteria mutations are unlikely to result in fundamental changes to membranes, this non-specific killing mechanism mitigates the development of resistance to HDPs.[7–10] Furthermore, the presence of a cationic charge enables HDPs to partially target anionic bacterial membranes over zwitterionic mammalian cell membranes, leading to reduced adverse effects on host cells.[11,12]

Although they have advantages over commercial antibiotics, the clinical applications of HDPs are restricted by their low bioavailability, low stability, and especially high manufacturing costs. These limitations may be addressed with synthetic antimicrobial polymers (AMPs), which mimic the structure of HDPs. Thanks to advancements in polymer chemistry, particularly reversible-deactivation radical polymerization and other techniques,[2,13–18] AMPs can be manufactured on a large scale for an economical cost and are less susceptible to proteolysis, leading to enhanced stability and bioavailability in biological environments.[11,19–22] Furthermore, by mimicking the structure and bactericidal mechanism of HDPs, antimicrobial polymers are also expected to kill bacteria by membrane disruption like HDPs,[7,9–11] thus preserving the advantages of HDPs over currently available antibiotics.

The development of AMPs is usually based on the principles of structure–activity relationships.[23,24] Numerous

Australian Centre for NanoMedicine and Cluster for Advanced Macromolecular Design (CAMD), School of Chemical Engineering, The University of New South Wales, Sydney, NSW 2052, Australia. E-mail: cboyer@unsw.edu.au

†Electronic supplementary information (ESI) available: Fig. S1–S19 and Table S1. See DOI: 10.1039/d1py01075a

researchers[12,23–27] have tried to identify the pivotal factors that can minimise the toxicity of AMPs to host cells without interfering with their antimicrobial effects. For the primary structure, most studies have found that amphiphilic balance and monomer design are important determinants in the bioactivity of AMPs. A good amphiphilic balance is necessary to enhance selectivity. Excessive hydrophobicity can lead to indiscriminate toxicity towards all cell types (including red blood cells), and may also induce protein complexation, reducing their therapeutic potency.[11,12,28,29]

A typical antimicrobial polymer contains cationic, and hydrophobic groups, and each of these components performs a specific role. The cationic groups facilitate the adsorption of the polymers onto the anionic bacterial membrane and affect the integrity of the cell membrane by interfering with the transport of compounds through the membrane.[7,9,11,12] Also, the interaction between the cationic groups and the cell membrane induces the polymers to adopt a globally amphiphilic conformation,[23] enhancing their bioactive performance. Recognising these crucial functions, many authors have investigated the impact of cationic groups on the overall bioactivity of AMPs.[26,30–32] Monomers functionalised with amino groups[19,26–28,30,31] and sulfonium bases[33–35] have been explored extensively as cationic choices. Judzewitsch *et al.*[30] and Palermo *et al.*[31] reported that amphiphilic copolymers containing primary amines display high antimicrobial activity against Gram-negative bacteria whereas those containing quaternary ammonium groups show more potency against mycobacteria (*Mycobacterium smegmatis).*[30] Meanwhile, Hirayama *et al.*[33] found that sulfonium compounds show higher potency against Gram-positive bacteria (*S. aureus*) than Gram-negative strains. Notably, for the first time, Hu *et al.*[34] introduced main-chain sulfonium-containing polymers with an AB-alternating sequence, showing excellent antibacterial effect against a broad-spectrum of clinically relevant bacteria strains. Alternatively, Ragogna and Gillies proposed phosphonium groups as potential choices to functionalise cationic monomers[32,36] Focusing on steric structure, Palermo *et al.*[26] introduced cationic side chain spacer arms as a new strategy design for modulating antibacterial activity and molecular conformation of random AMPs. In their polymer collection, the four carbon spacer arms in 4-amino-butylmethacrylate displayed the highest antimicrobial activity with minimum haemolytic activity.[26]

The second active component – the hydrophobic monomer, which directly inserts into and causes membrane disruption, has also gained considerable interest.[25,27,28,37] Libraries of polymers prepared with various types of hydrophobic monomers have been screened to elucidate the effect of its structure and induced global hydrophobicity on the overall selectivity of AMPs. Focusing on binary copolymers, Kuroda and co-workers investigated the effect of net hydrophobicity by correlating the bioactivity of poly(methacrylate) and poly(methacrylamide) derivatives with their hydrophobicity indicator or estimated partition coefficients (*i.e.*, $\log P$ calculated by their theoretical model based on the carbon atom number in the side chains, the mole fraction of hydrophobic groups and degree of polymerisation). The studies found that the haemolysis was directly proportional to the $\log P$ value.[25,27] Inspired by Kuroda's work, we have recently conducted a systematic investigation on the effect of hydrophobic groups on antimicrobial and haemolytic activity of ternary antimicrobial polymers.[28] With a library of 36 statistical amphiphilic polymers, we systematically evaluated the effect of monomer ratio, degree of polymerisation (DP_n), hydrophobic monomer carbon length, and chain type (cyclic, aromatic, linear, or branched) of the hydrophobic monomer on antibacterial and haemolytic activity. We found that minimising hydrophobicity and hydrophobic content was pivotal for modulating haemolytic activity while optimising antimicrobial activity required more complex factors, such as an appropriate cationic/hydrophobic balance and structural compatibility between the chosen components. Subsequent to this study, we selected the most promising polymers (*i.e.*, those with high antibacterial effects and low haemolysis) for further cytotoxicity testing. However, despite their high haemocompatibility, these polymers were still toxic towards mouse embryonic fibroblasts. This inspired us to continue optimisation through the present study to improve the selectivity of antimicrobial polymers by varying hydrophilic groups. As reported previously,[12,37–40] hydrophilic groups may reduce undesired protein complexation and haemolysis, thereby maintaining the antimicrobial activity of the polymers as well as conferring biocompatibility. Therefore, in this study, we synthesised a new collection of 20 antimicrobial polymers with varying types of hydrophilic and hydrophobic groups as well as their composition ratio to determine the effect of hydrophilic group structure and hydrophilic/hydrophobic balance on both the bioactivity and biocompatibility of antimicrobial polymers.

2. Materials and methods

Ethylenediamine (Sigma-Aldrich, ≥99%), *N*-isopentylamine (Sigma-Aldrich, 99%), *N*-hydroxyethyl acrylamide (HEAm) (Sigma-Aldrich, 97%), oligo(ethylene glycol) (PEG) methyl ether acrylate (number-averaged molecular weight (M_n) of 480 g mol^{-1}, Sigma-Aldrich), mPEG-acrylamide (molecular weight of 550 g mol^{-1}, Creative PEGWorks), 4-acryloylmorpholine (Sigma-Aldrich, 97%) triethylamine (TEA) (Scharlau, 99%), trifluoroacetic acid (TFA) (Sigma-Aldrich, 99%), RAFT agent (2-(*n*-butyltrithiocarbonate)-propionic acid, chloroform (Merck), dichloromethane (DCM) (Merck), tetrahydrofuran (THF) (Merck), diethyl ether, (Merck), hexane (Merck), dimethyl sulfoxide (DMSO) (Merck), dimethylacetamide (DMAc) (Sigma-Aldrich) and 5,10,15,20-tetraphenyl-21*H*,23*H*-porphine zinc (ZnTPP) (Sigma-Aldrich) were used as received. Deionised (DI) water was produced by a Milli-Q water purification system and had a resistivity of 17.9 mΩ cm^{-1}. The protected cationic monomer *tert*-butyl (2-acrylamidoethyl)carbamate (Boc-AEAm) and hydrophobic monomers (*N*-isopentylacrylamide, and *N*-benzylacrylamide) were synthesised according to the proto-

col reported in our previous study.[28] Red blood cells were provided by Serum Australis (Australia).

Synthesis of polymers

The statistical copolymers were synthesised using a slight modification of the general one-pot protocol reported previously.[30] Briefly, stock solutions of monomer were prepared with a concentration of 33 wt% in DMSO. RAFT agent 2-(*n*-butyltrithiocarbonate)-propionic acid (BTPA) was added to a 4 mL glass vial in an amount corresponding to the targeted DPn of 40. According to the targeted molar composition of copolymer, determined aliquots of monomer stock solutions were pipetted into the vial containing BTPA. DMSO was added to yield a final monomer concentration of 25 wt% in DMSO. ZnTPP photocatalyst (1 mg mL^{-1} in DMSO) was added at 100 ppm to monomer (ESI, Table S1†). The vial was sealed with a rubber septum and the headspace was deoxygenated with N_2 for 10 min in an ice-water bath. The vial was then placed under a green LED light (λ = 530 nm) for 20 h to produce the Boc-protected copolymers. The copolymers were analysed with SEC and NMR to examine the monomer conversion and other characteristics. Then, the polymer was purified by precipitation in a diethyl ether/hexane mixture (4 : 1) or (1 : 1) followed by centrifugation (9500 rpm for 3 min). The precipitate was dissolved in acetone and reprecipitated twice more. The polymer was then dried *in vacuo* prior to Boc group removal.

Deprotection

Trifluoroacetic acid (TFA) was used to remove Boc-protecting groups based on our group's previously reported protocol.[40] Briefly, polymer was dissolved in dichloromethane (~7 wt% polymer), followed by the addition of TFA (20 mol equivalent with respect to Boc groups). The mixture was stirred at room temperature for 3 h and precipitated into diethyl ether. The precipitate was isolated by centrifugation, dissolved in acetone and reprecipitated twice more. The polymer was then dried *in vacuo* and NMR analysis was used to determine the removal of Boc protective groups.

Characterisation

Characterisation of polymers in aqueous media. Dynamic light scattering (DLS) and zeta-potential measurements were performed using a Malvern Zetasizer Nano ZS apparatus equipped with a He–Ne laser operated at λ = 633 nm and at a scattering angle of 173°. All polymers were measured at a concentration of 1 mg mL^{-1} in DI water and the bacteria culture media (Mueller–Hinton broth, MHB).

For absorbance measurements, 200 μL of MHB solutions with or without polymers (1 mg mL^{-1}) was added to a 96-well microplate. The absorbance of the polymers in MHB at 595 nm was then measured using a microtiter plate reader (FLUOstar Omega, BMG Labtech).

^{1}H NMR spectroscopy. NMR spectroscopy was used to analyse polymer composition and conversion. All experiments were performed on a Bruker Avance III 300 MHz NMR spectrometer. All experiments were run with a gas flow across the probes at 535 L h^{-1} with sample spinning and at a temperature of 25 °C. Samples were dissolved in deuterated NMR solvents supplied by Cambridge Isotopes (DMSO-d_6) at concentrations of 10–20 mg mL^{-1}. Spectra were referenced to residual protons in the NMR solvent (DMSO-d_6: δ 2.50 ppm).

Size exclusion chromatography (SEC). SEC analysis was performed in DMAc [with 0.03% w/v LiBr and 0.05% 2,6-di-butyl-4-methylphenol (BHT)] at 50 °C and a flow rate of 1 mL min^{-1} with a Shimadzu modular system comprising an SIL-10AD automatic injector, a Polymer Laboratories 5.0 μL bead-size guard column (50 × 7.8 mm) followed by four linear PL (Styragel) columns (10^5, 10^4, 10^3, and 500 Å) and a RID-10A differential refractive-index detector. The system was calibrated using poly(methyl methacrylate) standards with molecular weights from 200 to 10^6 g mol^{-1}. Polymer solutions of 3 mg mL^{-1} were prepared in the eluent and filtered through 0.45 μm filters prior to injection.

Minimum inhibitory concentration (MIC)

The MIC of the prepared polymers was determined *via* the broth microdilution method in accordance with the Clinical and Laboratory Standards Institute (CLSI) guidelines.[41] The bacterial strains tested included three Gram-negative strains including wild-type *P. aeruginosa* PAO1 and multidrug-resistant strain PA37 (kindly provided by School of Optometry and Vision the University of New South Wales;[42,43] *Escherichia coli* (EC) K12; and a Gram-positive bacterium, *Staphylococcus aureus* (SA) ATCC 29213. Bacterial culture was grown overnight from a single colony in 10 mL of Mueller-Hinton broth (MHB) at 37 °C with shaking at 180 rpm. A subculture was prepared from the overnight culture by diluting 100 μL in 10 mL MHB and growing to mid-log phase (approximately 2.5 h), then diluted to *ca.* 1×10^6 cells per mL. A two-fold dilution series of 100 μL of polymer in MHB solution were added to a 96-well microplate followed by the addition of 100 μL of the subculture suspension. The final concentration of bacteria in each well was *ca.* 5×10^5 cells per mL. Positive controls without polymer and negative controls without bacteria or polymer were also included. The plates were then incubated at 37 °C for 20 h to ensure sufficient growth of inhibited bacteria, and the absorbance at 595 nm was measured with a microtiter plate reader (FLUOstar Omega, BMG Labtech). MIC values were defined as the lowest concentration of the sample that showed no visible growth and inhibited cell growth by more than 90% based on the broth microdilution method guided by CLSI.[41] The MIC endpoints are reported as the value of the lowest concentration if all replicates yielded the same value, or the concentration range if there was a difference between replicates. All assays included three replicates and were repeated in at least three independent experiments.

Haemolysis studies

Haemolytic activity of polymers was determined using fresh red blood cells (RBCs, provided by Serum Australis (Australia)) in accordance with previous protocol.[40] Briefly, RBCs were

diluted 1 : 20 in PBS (pH 7.4), pelleted by centrifugation (1000*g*, 10 min), and washed three times in PBS. The RBCs were then resuspended to achieve 5% (v/v) in PBS. Different concentrations of polymers (150 μL) were prepared in sterilised tubes, followed by addition of the 5% RBC suspension (150 μL). Polymer concentrations tested were 2000, 1000, 500, 250, 125, 62.5, and 31.25 μg mL^{-1}. PBS buffer was used as a negative control, and Triton-X 100 (1% v/v in PBS) was used as a positive haemolysis control. Tubes were incubated at 37 °C for 2 h with 150 rpm shaking. Samples were then centrifuged (1000*g*, 8 min), and 100 μL aliquots of supernatants were transferred into a 96-well microplate and absorbance values were read at 485 nm using a microtiter plate reader (FLUOstar Omega, BMG Labtech). Haemolysis percentage was calculated using the following equation:

$$\%\ \text{Haemolysis} = (A_{\text{polymer}} - A_{\text{negative}})/(A_{\text{positive}} - A_{\text{negative}}) \times 100\% \quad (1)$$

where A_{polymer} is the absorbance of the polymer treated supernatant, A_{negative} is the absorbance of the negative control and A_{positive} is the absorbance of the positive control. HC_{50} values, which are defined as the concentration of a compound required to cause 50% haemolysis, were calculated and reported as mean values with deviations based on the dose–response curve interpolated by GraphPad Prism version 8.4 for Windows (GraphPad Software). All experiments were performed in independent triplicates, each consisting of duplicates.

Cytotoxicity assay

The cytotoxicity of the polymer variations was tested using alamarBlue Assay (Thermo Fisher Scientific) on mouse embryonic fibroblasts (MEF) CF-1 (ATCC SCRC-1040), kindly provided by the Cell Culture Facility of the Mark Wainwright Analytical Centre (UNSW). MEFs were grown in complete medium (Dulbecco's Modified Eagle Medium (DMEM, Gibco), supplemented with L-glutamine (2 mM, Sigma-Aldrich), foetal bovine serum (FBS, 10% (v/v) and 1% penicillin/streptomycin (Sigma-Aldrich)), until reaching subconfluency at 37 °C and 5% CO_2 in a cell culture incubator (Eppendorf CellXpert® C170i). MEFs were used at passage numbers below 25 and were tested for mycoplasma contamination regularly. For the cytotoxicity assay, 100 μL cell suspension prepared at a concentration of 5×10^4 cells per mL in complete medium was seeded in 96-well plates and pre-incubated for 24 h at 37 °C and 5% CO_2. The complete media were replaced with 100 μL treatment medium (DMEM supplemented with 1% FBS, L-glutamine 2 mM and 1% penicillin/streptomycin) with polymers (treated samples) or without polymer (negative control). The 100% reduced form of alamarBlue Reagent, which was prepared by autoclaving a sample containing cell culture media and alamarBlue, was used as positive control. The cells were then incubated for 24 h at 37 °C and 5% CO_2. Subsequently, 10 μL of alamarBlue Assay Reagent (Thermo Fisher Scientific) was added to each well and incubated for 4 h at 37 °C. The fluorescence was measured (excitation 550 nm, emission 590 nm) using a microtiter plate reader (CLARIOstar® Plus, BMG Labtech). IC_{50} values, which are defined as the concentration of a compound required to cause 50% of its maximal inhibitory effect, were calculated and reported as mean values with deviations based on the dose–response curve interpolated by GraphPad Prism version 8.4 for Windows (GraphPad Software). All experiments were performed in independent triplicates, each consisting of duplicates.

3. Results and discussion

In this study, a collection of ternary amphiphilic copolymers was successfully prepared *via* oxygen-tolerant photoinduced electron/energy transfer-reversible addition–fragmentation chain transfer (PET-RAFT) polymerisation.[44–49] Based on the findings from our previous study, all polymers were prepared with a targeted degree of polymerisation (DP_n) of 40.[28] *tert*-Butyl (2-acrylamidoethyl) carbamate (Boc-AEAm) was employed as protected cationic monomer and was subsequently deprotected to reveal a primary amine after polymerisation. Four types of hydrophilic monomers, including (*N*-hydroxyethyl acrylamide (HEA), 4-acryloylmorpholine (AM), oligo(ethylene glycol) methyl ether acrylate (PEG-A), oligo(ethylene glycol) methyl ether-acrylamide (PEG-AA), and hydrophobic monomers, including (*N*-isopentyl acrylamide (I) and *N*-benzyl acrylamide (B)), as well as their molar ratio were investigated to determine their effect on the overall physicochemical and biological activity of the polymers. Based on the hydrophilic components, polymers were classified into two groups: the Non-PEG-group (including the polymers of AM and HEA-family) and the PEG-group (including the polymers of the PEG-A and PEG-AA-family). Polymers were named as F-H_{ab} where F and H value correspond to the type of the polymer family (either HEA, AM, PEG-A, or PEG-AA) and type of hydrophobic monomer, respectively, while a and b correspond to the targeted molar composition of the hydrophilic monomer and hydrophobic monomer, respectively. Recently, our group performed a high-throughput synthesis of antimicrobial copolymers and rapid evaluation of their bioactivity.[30] As reported, the hydrophobic-to-cationic ratio in the range of 20 : 80 up to 50 : 50 represents the highest antibacterial activity. In addition to that study, many other studies in our group[28,37,40,50] have confirmed that antimicrobial polymers containing 50% of the cationic group display good antimicrobial activity. From these previous studies, we decided to fix the molar composition of the cationic group at 50% for easier control and evaluation of the effect of hydrophilic and hydrophilic/hydrophobic balance on the bioactivity. Thus, the cationic molar composition was not included in the nomenclature.

Synthesis and characterisation of antimicrobial polymers

All the copolymers were prepared by the PET-RAFT method and were characterised by size exclusion chromatography

(SEC) and proton nuclear magnetic resonance spectroscopy (^{1}H NMR) analysis. The molecular weight distribution of all Boc-protected polymers was narrow as demonstrated by dispersity ($Đ$) values in the range of 1.06–1.17, which indicated good control of the polymerisations (Table 1). The number-averaged molecular weight (M_n) was estimated by SEC and ^{1}H NMR with good agreement between theoretical M_n and experimental values. The disappearance of vinyl proton signals at δ 5.5 and 6.3 ppm by ^{1}H NMR analysis of polymer mixtures prior to purification confirmed that the monomer conversions were over 99% for all polymers after 20-hour polymerisation (ESI, Fig. S1†).

^{1}H NMR analysis of purified polymers in HEA, PEG-A, and PEG-AA families exhibited good agreement between the monomer molar feed ratio and the purified copolymer molar composition (Table 1 & ESI, Fig. S2–S16†). The compositions of AM-polymers determined by ^{1}H NMR showed slightly greater deviations from the feed ratio (Table 1). In the final step of copolymer preparation, the Boc-groups were removed with trifluoroacetic acid (TFA) at room temperature for 3 h (Fig. 1B). The absence of the signal at δ 6.8 ppm (attributed to urethane group proton) and 1.4 ppm (attributed to *tert*-butyl group protons) in the ^{1}H NMR spectra of the polymers confirmed the successful removal of the Boc-protection group (ESI, Fig. S1†).

To determine if the monomers were preferentially incorporated in the polymer, we conducted kinetic studies of representative polymers (Fig. 2 & ESI, Fig. S19†). The monomers were statistically distributed within the polymer chain during the copolymerisation when acrylamides (PEG-AA-I2030) were used. In contrast, for copolymerisation involving acrylates (PEG-A-I2030), PEG-A was slightly more incorporated at the beginning of the polymerisation (Fig. 2 & ESI, Fig. S19†).

Aqueous characterisation of polymers

Representative polymers from each family were also characterised in aqueous media. All the characterised polymers had positive zeta potential (ζ) (+16–45 mV) owing to the cationic charge of the amino groups (Table 1). The presence of cationic amino and hydrophobic groups in antimicrobial polymers may induce the formation of so-called polymer–protein complexes (PPCs) *via* electrostatic and hydrophobic interactions between polymers and protein in biological media like the bacteria cell culture media (MHB).[37–39,51,52] PPC formation can lead to reduced antimicrobial activity as the cationic groups are prevented from complexing with the anionic bacterial membranes.[37,53] To get an indication of the extent of PPC formation, DLS analysis, absorbance measurements at 595 nm, and visual inspections were performed in both DI water and MHB (Table 1). In DI water, no turbidity was observed for any polymer and all polymers were poorly detected by DLS at a concentration of 1 mg mL^{-1}, showing that the polymers did not form large aggregates and were completely soluble. However, in MHB, some polymers formed PPCs as evidenced by the detection of the increased hydrodynamic particle size (D_h) measured by DLS, the solution turbidity observed visually, and by the significantly increased absorbance measurements. None of the PEG-polymers formed PPCs regardless of composition ratio, which is in accordance with our previous report.[37] HEA-polymers generally did not form PPCs except for those polymers with a very low hydrophilic/hydrophobic ratio (HEA-I1040) whereas AM-polymers did. This is consistent with previous research from our group, which showed that increasing hydrophilic balance reduced PPC formation and improved antimicrobial activity.[28,37]

Antimicrobial activity

The minimum inhibitory concentration (MIC), or the lowest concentration of polymer that inhibits visible growth was used to evaluate the antimicrobial activity of the polymers against four bacterial strains: three Gram-negative strains, including wild-type *P. aeruginosa* PAO1 and multidrug-resistant strain PA37; *Escherichia coli* (EC) K12; and a Gram-positive bacterium, *Staphylococcus aureus* (SA) ATCC 29213.

Firstly, we investigated the MIC of our polymers against the different bacterial strains. Pleasingly, the majority of polymers tested showed good efficacy against the Gram-negative strains, including the MDR PA37. Although PA37 appeared to be slightly less sensitive to most tested polymers than PAO1 and K12, the low MICs recorded demonstrated that the polymers were generally still effective against this strain, suggesting the polymers have potential to combat the multidrug-resistant Gram-negative pathogen.[54,55] Consistent with our previous findings, the polymers were almost inactive against Gram-positive bacteria (Fig. 3). The difference in activity of the polymers against Gram-negative and Gram-positive bacteria can be attributed to the difference in the structure of their cell walls, which was explained in our previous publication.[28] Therefore, the target bacterial strain is an important factor to consider when designing antimicrobial polymers. In this study, we focused on Gram-negative pathogens because no new classes of antibiotics have been approved for Gram-negative pathogens for over 50 years despite their rising dangerous multidrug resistance.[2–4]

In our previous study, we found that the I family (the polymers containing *N*-isopentyl acrylamide – the mimic structure of amino acid leucine) displayed the highest antibacterial effect, whereas the B family (the polymers containing benzyl acrylamide) exhibited the lowest haemolysis.[28] Therefore, in this study, either *N*-isopentyl acrylamide (I) or benzyl acrylamide (B) was selected as the hydrophobic monomer to copolymerise with other components. Also, in the active range of both I and B-polymers, the content of hydrophobic group was directly proportional to the antibacterial effect. The present study was consistent with the previous findings that, regardless of varying hydrophilic types, I-polymers show a higher antibacterial effect than B-polymers; and increasing the hydrophobic content improved the antibacterial effect (Fig. 3). Therefore, we mainly investigated the I-polymers to evaluate the effect of tuning the hydrophilic group and hydrophilic/hydrophobic ratio on the antibacterial effect.

Table 1 Polymer characterisation by ^{1}H NMR, SEC and DLS analyses

Group of polymers	Family of polymers	Polymer	Feed ratio (cationic : hydrophilic : hydrophobic) (mol%)	Composition[a] cationic : hydrophilic : hydrophobic (mol%)	Theo. M_n [b] (g mol^{-1})	$M_{n,SEC}$ [c] (g mol^{-1})	$M_{n,MNR}$ [d] (g mol^{-1})	$Đ$[c] (nm)	D_h (nm) in MHB[e]	PDI in MHB[e]	ζ in DI water[e] (mV)	Absorbance[f]
Non-PEG group	HEA-family	HEA-I1040	50 : 10 : 40	51 : 10 : 39	7200	11 500	9800	1.1	173	0.1	22.5	0.10
		HEA-I1535	50 : 15 : 35	50 : 17 : 33	7200	11 700	8700	1.06	—	—	18.9	0.10
		HEA-I2030	50 : 20 : 30	52 : 20 : 28	7100	8800	8200	1.13	—	—	27.9	0.07
		HEA-I3020	50 : 30 : 20	53 : 31 : 16	7000	6800	7100	1.15	—	—	nd	nd
		HEA-B1040	50 : 10 : 40	51 : 10 : 38	7600	11 700	nd	1.11	—	—	33.6	nd
		HEA-B1535	50 : 15 : 35	52 : 15 : 33	7500	11 900	nd	1.1	—	—	15.5	nd
	AM-family	AM-I1535	50 : 15 : 35	56 : 15 : 29	7300	9900	8400	1.1	nd	nd	nd	nd
		AM-I2030	50 : 20 : 30	52 : 17 : 31	7300	10 000	8100	1.08	216	0.13	44.5	0.07
		AM-I3020	50 : 30 : 20	51 : 26 : 22	7300	10 000	8100	1.1	nd	nd	nd	0.07
		AM-B1040	50 : 20 : 30	nd	7700	10 000	nd	1.13	229	0.08	27.1	0.54
		AM-B1535	50 : 15 : 35	54 : 12 : 34	7600	9500	9000	1.1	217	0.08	23.8	0.70
PEG group	PEG-AA-family	PEG-AA-I1040	50 : 10 : 40	50 : 11 : 39	9000	14 400	8900	1.15	—	—	23.7	0.07
		PEG-AA-I1535	50 : 15 : 35	48 : 16 : 36	9800	15 500	11 100	1.17	—	—	33.9	0.08
		PEG-AA-I2030	50 : 20 : 30	48 : 21 : 31	10 600	15 800	12 800	1.17	—	—	24.1	0.07
	PEG-A-family	PEG-A-I1040	50 : 10 : 40	50 : 10 : 39	8700	11 800	8400	1.13	—	—	39.3	0.07
		PEG-A-I1535	50 : 15 : 35	48 : 15 : 37	9400	11 100	11 000	1.1	—	—	44.5	0.07
		PEG-A-I2030	50 : 20 : 30	49 : 21 : 31	10 100	11 500	12 600	1.13	—	—	22.5	0.07
		PEG-A-I3020	50 : 30 : 20	49 : 29 : 22	11 400	11 600	11 500	1.15	—	—	nd	0.07
		PEG-A-B1040	50 : 10 : 40	52 : 11 : 37	9000	11 000	8300	1.13	—	—	31.7	0.10
		PEG-A-B1535	50 : 15 : 35	51 : 16 : 33	9700	11 000	13 300	1.13	—	—	20.6	0.10

[a] Composition calculated by NMR. [b] Theoretical molecular weight calculated using feed ratios and full monomer conversion (see ESI†) before Boc-deprotection. [c] Determined *via* SEC analysis of copolymers before Boc-deprotection in DMAc solvent. [d] Molecular weight calculated by NMR using the experimental copolymer composition in the copolymers (see ESI† for additional information). [e] Determined by Malvern Zetasizer Nano ZS apparatus after Boc-deprotection at a concentration of 1 mg mL^{-1}. [f] Absorbance measured at 595 nm in MHB after Boc-deprotection at a concentration of 1 mg mL^{-1}. Note: (—) no large aggregate, (nd) – not determined.

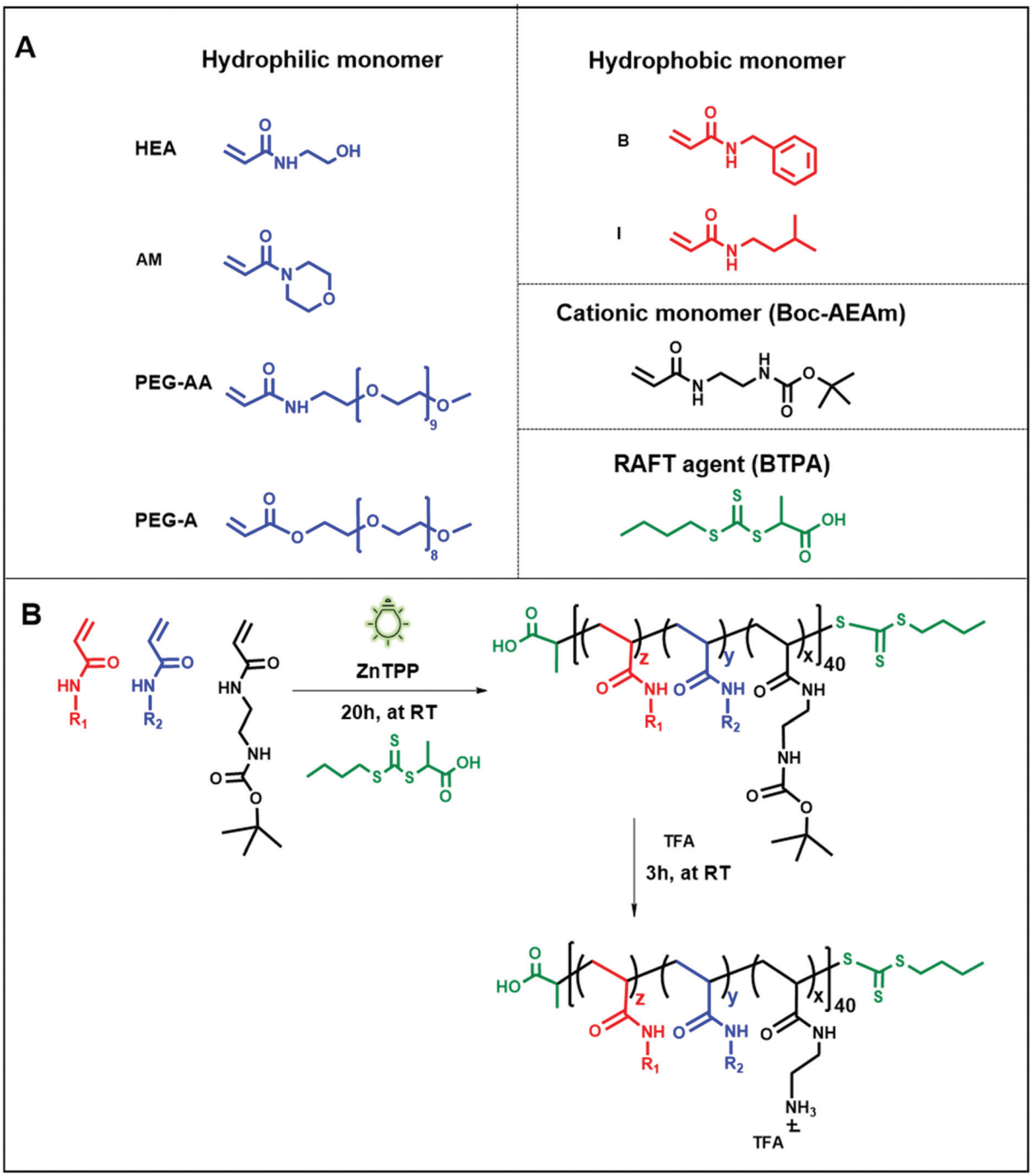

Fig. 1 (A) Key reagents used in this study. Chemical structures of cationic monomer: *tert*-butyl (2-acrylamidoethyl) carbamate (Boc-AEAm), hydrophilic monomer: hydroxyethyl acrylamide (HEAm), 4-acryloylmorpholine (AMm), poly(ethylene glycol) methyl ether acrylate (PEG-A), and mPEG-acrylamide (PEG-AA), hydrophobic monomers: *N*-isopentylacrylamide (I) and *N*-benzylacrylamide (B) and RAFT agent: 2-(*n*-butyltrithiocarbonate)-propionic acid (BTPA). (B) Reaction scheme for the synthesis of antimicrobial polymers by PET-RAFT polymerisation. R_1, R_2 is hydrophobic or hydrophilic chain, respectively.

Overall, the AM-family showed the highest Gram-negative antibacterial effect. Particularly, with a similar hydrophilic/hydrophobic ratio, the MIC_{PA01} (MIC values against PA01) of AM-I1535 (8–16 μg mL^{-1}) and AM-I2030 (16 μg mL^{-1}) were lower than all corresponding polymers in other families (16 μg mL^{-1} and 16–32 μg mL^{-1} for HEA/PEG-A/PEG-AA-I1535 and HEA/PEG-A/PEG-AA-I2030, respectively). Notably, despite a small hydrophobic portion, AM-I3020 inhibited both PA strains at a concentration of 64 μg mL^{-1}, whereas other family members with the same composition (HEA/PEG-A-I3020) were inactive against both PA strains at any concentration in the tested range. This could result from the higher global hydro-

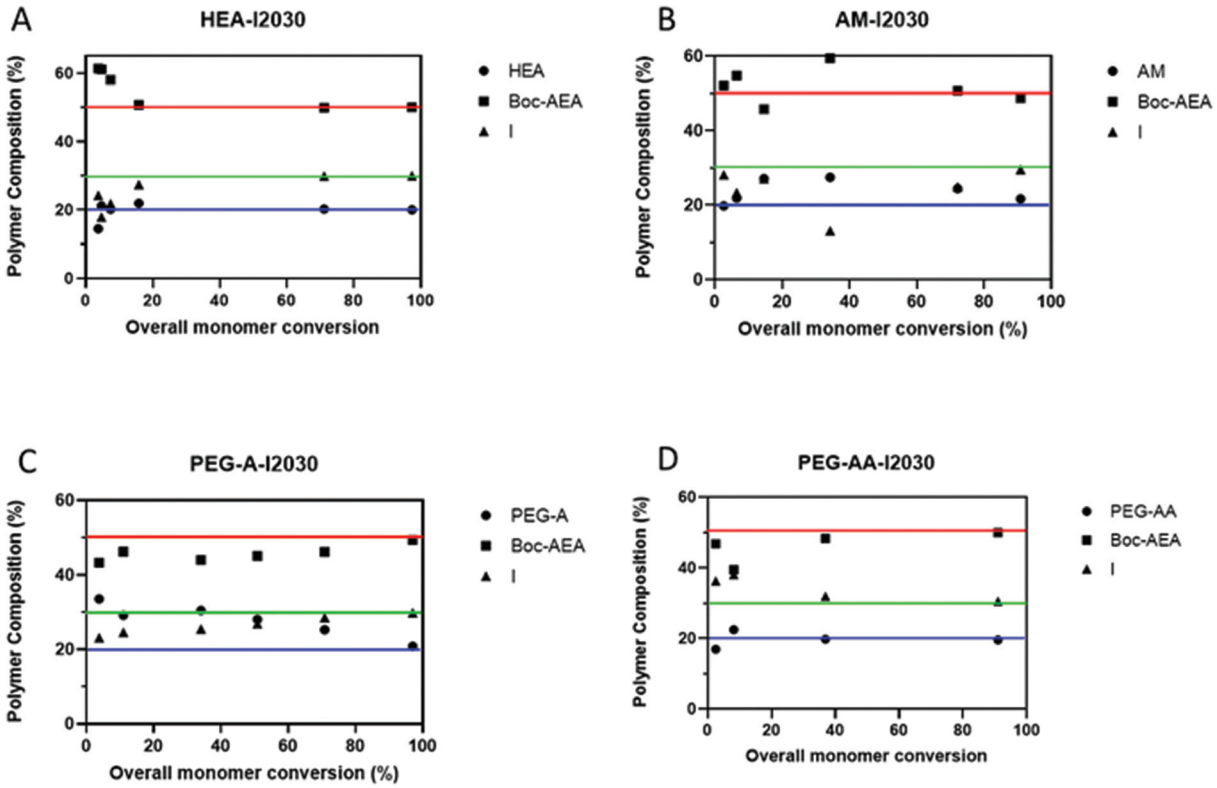

Fig. 2 Molar polymer composition at different overall monomer conversions for (A) HEA-I2030, (B) AM-I2030, (CPEG-A-I2030 and (D) PEG-AA-I2030 copolymers. Coloured horizontal lines show expected composition based on monomer feed ratio.

phobicity of AM-polymers compared with other families due to the significantly lower hydrophilicity of the AM group, illustrated by the homo-tetramer's Clog *P* (a theoretical partition coefficients calculated by Chemdraw (version 18.1 and 19.0) software) (Table 2).

PEG-A and PEG-AA families showed a similar trend in aqueous behaviour and bioactivity. This can be explained by their long PEG chains. The hydrophilicity of PEG is due to the presence of ether oxygen atoms (–O–) in the ethylene oxide units, which can interact with water by forming numerous hydrogen bonds.[56,57]

Additionally, PEG-A and PEG-AA families displayed similar antibacterial activity to the HEA-family, except for the polymers with a very low hydrophilic/hydrophobic ratio (PEG-A/PEG-AA/HEA-I1040), which can be attributed to their different properties in aqueous media. In contrast to HEA-I1040, all prepared polymers in the PEG and HEA-families did not form polymer–protein complexes (PPCs). Our previous study indicated that both the overall hydrophobicity and chain length of hydrophobic groups impact PPC formation.[28] Owing to higher hydrophobicity, the PPC formation induced by HEA-I1040 might reduce its antibacterial activity, leading to its higher MIC_{PA01} value (16 μg mL^{-1}) compared with the MIC_{PA01} of PEG-A/PEG-AA-I1040 (8 μg mL^{-1}) (Fig. 3 & Table 2). In agreement with previous research in our group, a hydrophilic component, and especially a highly hydrophilic one like PEG might increase hydrophilic balance and mask the positive charges, reducing PPC formation and thereby enhancing antimicrobial activity.[28,37]

In summary, the hydrophilic group is not an active component that is directly involved in membrane disruption; however, it indirectly affects the overall antibacterial activity through changing the net hydrophobicity and the aqueous characteristics of polymers and preventing PPC formation in *in vitro* conditions.

Biocompatibility and selectivity

In this study, the biocompatibility of antimicrobial polymers was evaluated by determining the toxicity of polymers to mammalian cells using sheep red blood cell and mouse embryonic fibroblasts (MEFs). Looking firstly at red blood cells, as shown in Fig. 4, in the same family, the hydrophobic monomer content of the copolymer was directly proportional to the HC_{50} value, which is defined as the concentration of a compound required to cause 50% haemolysis. Also, owing to their lower hydrophobicity, B-polymers induced less haemolysis than I-polymers. For example, with the highest hydrophobic content (40%), in the HEA-family, HEA-I1040 caused substantial haemolysis at a lower concentration (HC_{50} of ~142 μg mL^{-1}) than HEA-B1040 (HC_{50} of ~961 μg mL^{-1}). Similarly, in the PEG-A family, PEG-A-I1040 (HC_{50} of ~500 μg mL^{-1}) induced significantly more haemolysis than PEG-A-B1040 (HC_{50} of ~1563 μg mL^{-1}).

Group	Family	Polymer	Target monomer Ratio (a)	MIC (μg/mL)			
				PA		EC	SA
				PA01	PA37	K12	29213
Non-PEG group	HEA	HEA-I1040	50:10:40	16	nd	16	>256
		HEA-I1535	50:15:35	16	32	16	>256
		HEA-I2030	50:20:30	16-32	32-64	32	>256
		HEA-I3020	50:30:20	>256	>256	>256	>256
		HEA-B1040	50:10:40	16-32	nd	32	256
		HEA-B1535	50:15:35	32-64	nd	64-128	>256
	AM	AM-I1535	50:15:35	8-16	16-32	16	>256
		AM-I2030	50:20:30	16	32	16	>256
		AM-I3020	50:30:20	64	64	64-128	>256
		AM-B1040	50:10:40	32	32-64	32-64	nd
		AM-B1535	50:15:35	32	32-64	32-64	nd
PEG group	PEG-AA	PEG-AA-I1040	50:10:40	8	16-32	8-16	>256
		PEG-AA-I1535	50:15:35	16	32	8-16	>256
		PEG-AA-I2030	50:20:30	16-32	32-64	32	>256
	PEG-A	PEG-A-I1040	50:10:40	8	16-32	8-16	>256
		PEG-A-I1535	50:15:35	16	32-64	8-16	>256
		PEG-A-I2030	50:20:30	16-32	64-128	32-64	>256
		PEG-A-I3020	50:30:20	>256	>256	>256	>256
		PEG-A-B1040	50:10:40	16-32	32-64	32-64	nd
		PEG-A-B1535	50:15:35	32-64	64	64-128	nd

Fig. 3 Antimicrobial activity (minimum inhibitory concentration (MIC)) of polymers against Gram-negative strains, including wild-type *P. aeruginosa* PAO1 and multidrug resistant strain PA37; *Escherichia coli* (EC) K12; and Gram-positive bacteria, *Staphylococcus aureus* (SA) ATCC 29213. Note: a – molar feed ratio: cationic : hydrophilic : hydrophobic.

Next, the effect of the hydrophilic group on the haemolytic activity was investigated by comparing representatives from each family. Generally, the PEG-group polymers showed greater haemocompatibility than the Non-PEG-group polymers. For example, based on the haemolysis induced by polymers with the highest hydrophobic content (40%), the PEG-polymers (PEG-A/PEG-AA-I1040) showed ~3 times greater haemocompatibility than HEA-I1040. Furthermore, with the same polymer composition (molar ratio of cationic/hydrophilic/hydrophobic equal to 50 : 20 : 30), in the tested concentration range, AM-I2030 induced moderate haemolysis (HC_{50} of ~1505 μg mL^{-1}) while the corresponding polymers in other families (HEA/PEG-A/PEG-AA-I2030) did not (HC_{50} of >2000 μg mL^{-1}). Similarly, for the B-hydrophobic group, AM-B1535 (HC_{50} of ~855 μg mL^{-1}) was more haemotoxic than either HEA-B1535 or PEG-A-B1535 (HC_{50} > 2000 μg mL^{-1}). In summary, the polymers displayed different haemocompatability according to the hydrophilic group, which followed this specific order: PEG-AA ~ PEG-A > HEA > AM.

To further evaluate the cytotoxicity of the polymers, the viability of mouse embryonic fibroblasts (MEFs) after 24 h treatment with the polymers was assessed with the alamarBlue assay, which is a well-established technique for determining cell viability.[58–61] The cytotoxicity by alamarBlue assay followed the general trends of haemolytic activity, namely: (1) the polymers inducing substantial haemolysis were also highly toxic to MEFs; (2) increasing net hydrophobicity by increasing hydrophobic content led to increased cytotoxicity against MEF. For example, in the PEG-AA family, as the ratio of hydrophobic content increased from 30% to 35% to 40%, the half-maximal inhibitory concentration (IC_{50}) decreased from 512 to 166 to 43 μg mL^{-1}, respectively. It is noteworthy that IC_{50} is a widely used measure to determine the biocompatibility of a compound.[62] However, IC_{50} values obtained by alamarBlue assay were significantly lower than HC_{50} values based on haemolysis, suggesting a narrower range of biocompatible polymers (Fig. 4). A possible explanation for the difference might be the different experimental conditions and cell types.[63] Particularly, some haemocompatible polymers (HC_{50} > 2000 μg mL^{-1}) such as HEA-I1535 and HEA-B1535 inhibited the growth of MEFs at substantially lower concentrations (IC_{50} of ~29 ± 4 and 43 ± 3 μg mL^{-1}, respectively). Most polymers were quite toxic to

Table 2 Length of hydrophilic spacer arm/pendant group

Pendant group		Structure of Pendant group	Length of hydrophilic spacer arm/pendant group[a] (Å)	Clog P[b]
Cationic monomer			4.9	−2.39
Hydrophilic monomer	HEA	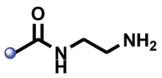	4.8	−2.69
	AM	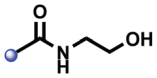	4.2	0.75
	PEG-AA	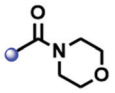	27.2	−5.96
	PEG-A	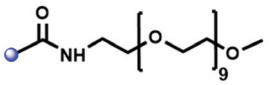	24.8	−3.04
Hydrophobic monomer	I	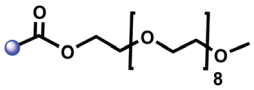	6.2	6.57
	B	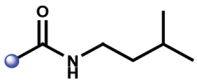	6.3	6.18
		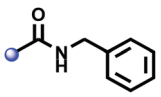		

[a] The measurement was based on Chem3D software. For the hydrophobic or cationic monomer, the length of the pendant group was measured from the carbonyl group carbon to the end group. For the hydrophilic monomer, the length of the hydrophilic spacer arm was measured from the carbonyl group carbon to the end (O). [b] A theoretical Clog P calculated using a DPn of 4 (Chemdraw (version 18.1 and 19.0) software).

MEFs at low concentrations (around 50 μg mL^{-1}), and some polymers, such as HEA-I2030, AM-I3020, PEG-AA-I1535, and PEG-A-I1535, were moderately toxic with 2–3 times higher IC_{50} values. Additionally, as shown in Fig. 5, polymers in the two families of PEG group polymers shared a similar trend in cytotoxicity and were less toxic than Non-PEG group polymers. Especially, PEG-AA-I2030 and PEG-A-I2030 were highly biocompatible with an IC_{50} of >512 μg mL^{-1}, which was much higher than the IC_{50} of HEA/AM-polymers with the same composition ratio (HEA-I2030 and AM-I2030 with IC_{50} of ~122 μg mL^{-1} and ~56 μg mL^{-1}, respectively).

Next, to estimate the selectivity of polymers toward Gram-negative bacteria and mammalian cells, the therapeutic index (TI) was calculated by dividing the value of IC_{50} by the value of MIC (against wild type PA01). An optimised hydrophilic/hydrophobic ratio improved the selectivity of synthetic polymers toward bacteria than mammalian cells. For example, the PEG-AA/PEG-A/HEA-I2030 (TI of 21.3, 21.3, and 5.1, respectively) showed higher selectivity than their relatives with more hydrophobic content, such as PEG-AA-I1040 (TI of 5.4), PEG-A-I1040 (TI of 4.9), HEA-I1535 (TI of 1.8). Also, coinciding with the trend of cytotoxicity against MEFs, the PEG group polymers displayed higher selectivity than the Non-PEG group. We hypothesised that a possible explanation might be attributed to the PEG's flexible chain length and high hydrophilicity affecting the aqueous characteristics in protein-rich media of the polymers and their globally amphiphilic conformation on the cell membrane (*vide infra*).

Owing to the amphiphilic nature of antimicrobial polymers in aqueous media, like the amphiphilic polypeptides, the polymers tend to adopt a random conformation, in which the hydrophobic groups tend to clump together to minimise contact with water, self-assembling to create hydrophobic pockets.[64,65] In contrast, the hydrophilic and cationic groups tend to distribute themselves outward to interact with

Group	Family	Polymer	HC_{50} (μg/mL)	IC_{50} against MEF (μg/mL)	TI (IC_{50})
Non-PEG group	HEA	HEA-I1040	142 ± 6	nd	nd
		HEA-I1535	nd	29 ± 4	1.8
		HEA-I2030	>2000	122 ± 19	5.1
		HEA-I3020	>2000	nd	nd
		HEA-B1040	961 ± 425	59 ± 37	2.5
		HEA-B1535	>2000	43 ± 3	0.9
	AM	AM-I1535	1825	56 ± 13	4.7
		AM-I2030	1505 ± 29	56 ± 15	3.5
		AM-I3020	>2000	326 ± 101	5.1
		AM-B1040	878 ± 81	39 ± 25	1.2
		AM-B1535	855 ± 212	36 ± 7	1.1
PEG group	PEG-AA	PEG-AA-I1040	390 ± 87	43 ± 10	5.4
		PEG-AA-I1535	>2000	166 ± 17	10.4
		PEG-AA-I2030	>2000	~512	21.3
	PEG-A	PEG-A-I1040	500 ± 343	39 ± 2	4.9
		PEG-A-I1535	>2000	130 ± 30	8.1
		PEG-A-I2030	>2000	~ 512	21.3
		PEG-A-I3020	>2000	>512	nd
		PEG-A-B1040	1563 ± 135	56 ± 7	2.3
		PEG-A-B1535	>2000	191 ± 30	4

Higher biocompatibility

Fig. 4 Overall biocompatibility and selectivity of polymers. Biocompatibility of polymers was evaluated by determining their haemolytic activity to sheep red blood cells and their toxicity to mouse embryonic fibroblasts (MEFs) using alamarBlue assay based on measuring metabolic activity of the viable MEFs. The selectivity of polymers was evaluated by therapeutic index (TI) of polymers which were calculated as the ratio between IC_{50} (against MEFs) and MIC (against wild type PA01). Note: for the calculation of TI, if a MIC range was reported, we used the average MIC value.

water,[66,67] creating a hydration interface between the polymer and aqueous media (Fig. 6).

Notably, the structure of hydrated water around polymers has been considered a key factor responsible for the biocompatibility of polymers. From the surface of a biocompatible polymer, water presents in the following layers: tightly bound water (non-freezing water) → loosely bound water (intermediate water) → free water.[70,71] The hydrated multi-layered structure, especially the layers of tightly bound water[37,72] and intermediate water,[70,71] creates a protective physicochemical shield to prevent the interactions between hydrophobic and cationic groups and the biocomponents, such as proteins or cell membranes. It is important to note that owing to the presence of cationic charged and hydrophobic groups, the amphiphilic antimicrobial polymers may easily trigger undesirable protein complexation in the physiological environment, leading to a loss in antimicrobial potency as well as induction of adverse effects for these biocomponents through electrostatic and hydrophobic interactions.[37–39,51,52] Therefore, developing a protective hydrated shell by optimising hydrophilic components with sufficient thickness, density, and flexibility is necessary to minimise cytotoxicity toward the host cells without interfering with their activity against the target pathogen.

Over recent decades, PEG has been the commonly used as non-ionic hydrophilic polymer with stealth behaviour and has been widely employed in the food, cosmetic and pharmaceutical industry owing to its high biocompatibility.[72,73] Incorporating PEG in bioactive compounds profoundly influences cell behaviour at different levels. For instance, at *in vitro* level, PEGylation improves the aqueous solubility of materials, thus preventing their aggregation in aqueous media; and avoids unwanted protein complexation in *in vitro* media, thus preserving their bioactivity.[56,74] At *in vivo* level, the PEGylation minimises opsonisation, thus reducing adverse immunological effects; prolongs circulatory time by reducing renal clearance; thereby improving their overall efficacy.[72] Herein, we focus on the *in vitro* level to study how PEG significantly improved the TI value of PEG-group polymers over HEA/AM-polymers.

Compared with the Non-PEG hydrophilic types (AM and HEAm), the PEG-A and PEG-AA are much more hydrophilic as

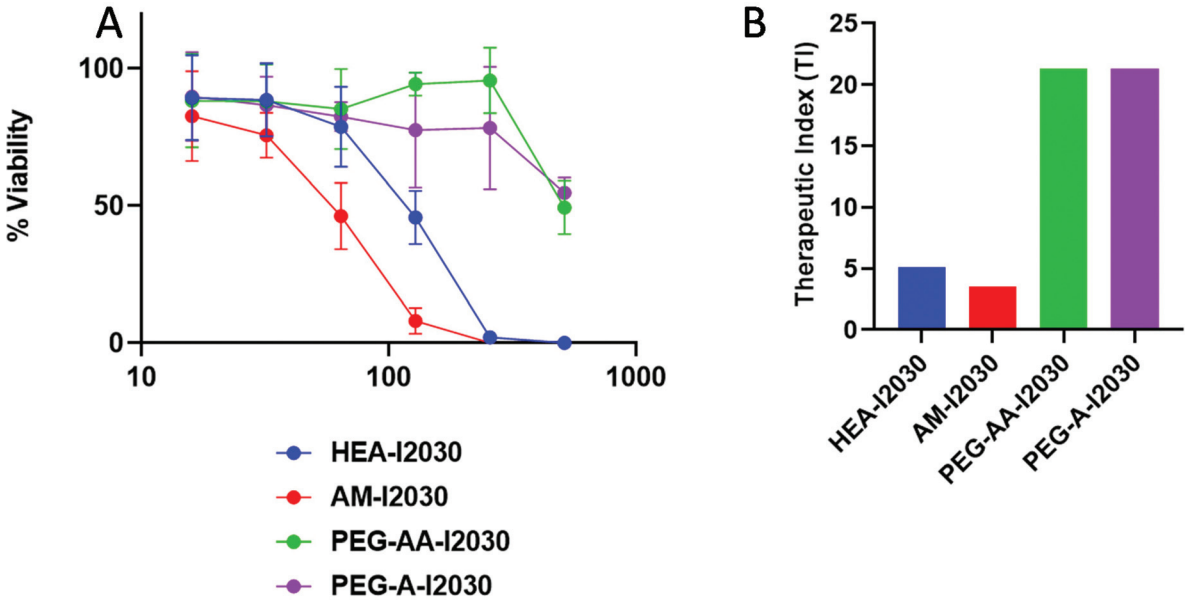

Fig. 5 (A) The viability of MEFs at 24 h post-treatment with representative polymers at different concentrations. (B) Therapeutic index of representative polymers. Biocompatibility of polymers was evaluated by determining their toxicity to mouse embryonic fibroblasts (MEFs) using alamarBlue assay based on measuring metabolic activity of the viable MEFs. The selectivity of polymers was evaluated by therapeutic index of polymers which were calculated as the ratio between IC_{50} (against MEFs) and MIC (against wild type PA01).

demonstrated by Clog*P* values <−3 (Table 2) and flexible. Owing to repeated ethylene glycol subunits with many ether (–O–) groups distributed evenly along the chain, the PEG side chain may form numerous hydrogen bonds with water molecules. Consequently, they may create a denser hydration layer (also called conformational cloud or sphere)[56,57,70–72,74] than AM/HEA groups (Fig. 6). To estimate the hydrodynamic radius of the hydrated sphere, the hydrophilic spacer arms (distance from the carbonyl group carbon to the last –O–/–OH– end group of hydrophilic pendants) were computed by Chem3D software. As shown in Table 2, interestingly, the hydrophilic spacer arm of the AM pendant (d = 4.2 Å) is slightly shorter than the length of both cationic (d = 4.9 Å) and hydrophobic groups (d = 6.2 Å, 6.3 Å for I and B pendants, respectively). The short AM/HEA groups might be insufficient to mask the cationic charges and hydrophobic groups, which ineffectively hinder these groups to interact *via* electrostatic or hydrophobic interactions with protein present in the media. In addition, in contact with mammalian cells, these polymers can strongly interact with these membranes, resulting in the formation of amphiphilic conformation (Fig. 6). By contrast, the hydrophilic spacer arm of the PEG-A/PEG-AA side chain is much longer (d = 24.8 Å, 27.2 Å for PEG-A and PEG-AA, respectively) than hydrophobic and cationic groups (Table 2), which prevents the formation of interactions with proteins and mammalian cells (Fig. 6). The flexibility of the water-soluble chain also influences the density of the conformational cloud.[75,76] Torchilin *et al.*[75] highlighted the critical role of flexibility (conformational mobility) of water-soluble polymer chains in the conformational cloud. A relatively small number of water-soluble but highly flexible polymer molecules can create a sufficient number of high-density conformational "clouds" to hinder the cationic and hydrophobic groups, limiting their interactions with other compounds (Fig. 6).[75] For instance, PEG-A/PEG-AA-I1040 did not form PPCs in MHB despite having the lowest amount of hydrophilic content (10% molar), whereas AM-I2030 was unable to avoid PPC formation, despite double the hydrophilic content (20% molar).

The antimicrobial polymers start to adopt a globally amphiphilic conformation in contact with highly negative bacterial membranes (Fig. 6).[23,68,69] This adoption is triggered by strong electrostatic interactions between the highly negative bacterial outer membrane and the cationic groups. The amphiphilic polymers tend to organise their structure to maximise the contact area of the cationic parts over the bacterial cell surface while exposing hydrophilic parts toward the aqueous media due to its hydrophilic nature (Fig. 6). As a result, the protective hydration layer in the polymer–membrane interface is impaired, enabling the hydrophobic interaction between uncovered hydrophobic parts of polymers and the bilipid membrane and, subsequently, causing membrane disruption. This process likely depends mainly on the strength of electrostatic and hydrophobic interactions between active components of polymers and bacterial membrane surfaces. Garima Rani *et al.*[66,67] investigated by detailed atomistic simulations the incorporation of hydrophilic groups within antimicrobial polymer chains. The incorporation of hydrophilic groups limits the interactions between the hydrophobic groups which prevents the formation of aggregates in aqueous media and increases their availability to interact with bacterial membrane.

However, this adoption may proceed in various manners as the amphiphilic polymers contact the mammalian membrane.

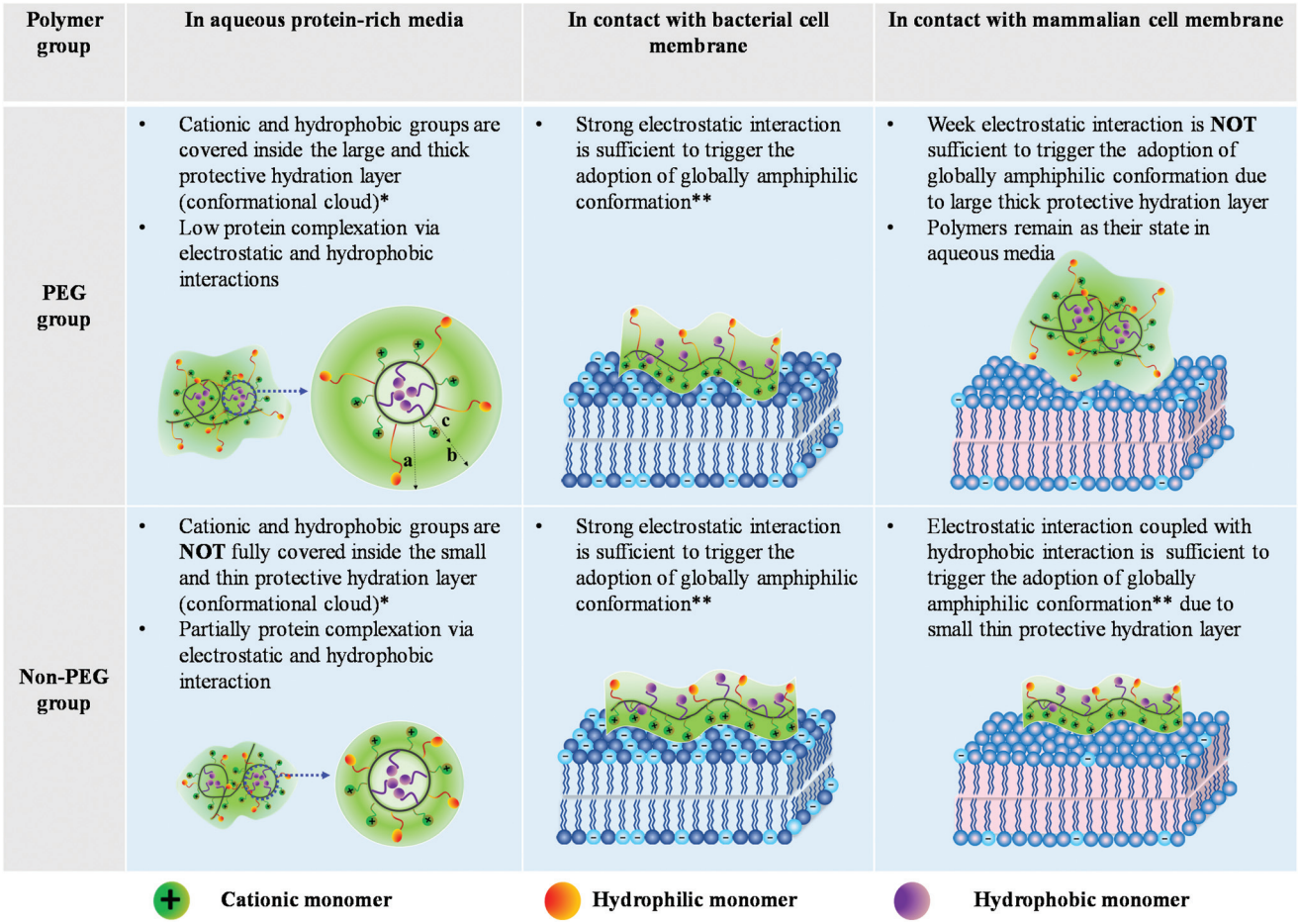

Fig. 6 Proposed adoption of PEG group polymer and Non-PEG group polymer in protein-rich media and in contact with bacterial and mammalian cell membranes. (*) Protective hydration layer (conformational cloud) polymer: (a) is hydrodynamic radius of hydrated polymer; (b) and (c) are layers of intermediate water (loose bound water) and tightly bound water respectively. (**) Owing to different lipid topologies, bacterial and mammalian membranes are characteristically different in charge.[23,68,69] The amphiphilic polymer tends to organise its composition to maximise the contact area of the cationic part over the bacterial cell surface while exposing the hydrophilic parts toward the aqueous media. Owing to hydrophobic interaction, the hydrophobic parts of polymers tend to insert into the bilipid membrane leading to membrane disruption.

Owing to its different structure and composition, the mammalian cell membrane is more zwitterionic (or less negatively charged) than the bacterial cell membrane, leading to a weaker electrostatic attraction to the cationic groups of the polymers (Fig. 6). This critical factor determines the selectivity of cationic polymers toward bacteria over the mammalian cells.[23,68,69] However, not only electrostatic, but also hydrophobic interactions have an essential role in this process. Herein, two groups of polymers demonstrated two typical cases.

For PEG-group polymers in contact with mammalian cells, the weaker electrostatic attraction between the two oppositely charged sides appears to be not strong enough to break the thick firm protective hydration barrier that triggers the globally amphiphilic conformation (Fig. 6). PEG-polymers were probably insulated in a protective hydration sphere until accumulating a sufficient concentration threshold to impair the blood/MEF cells. By contrast, for the Non-PEG group, particularly AM-polymers, the protective hydration barrier was weaker; and the electrostatic and hydrophobic interactions between the polymer and mammalian cell membrane components were stronger owing to their shorter distance. As a result, the AM-polymer might require a lower threshold concentration to break the hydration barrier to induce the globally amphiphilic conformation that disrupts the mammalian cell membrane (Fig. 6).

To sum up, in agreement with Tanaka *et al.*,[70,71] we hypothesised that water structure bound around the polymer surface has an essential role in aqueous behaviour that significantly affects the antibacterial activity and, especially, the biocompatibility of AMPs. Altogether, PEG-polymers were more compatible with tested mammalian cells and more selective at targeting Gram-negative bacteria than AM/HEA-polymers. In particular, PEG-AA-I2030 and PEG-A-I2030, showed not only high antibacterial effects (MIC of 16–32 μg mL^{-1}) but also high biocompatibility (HC_{50} > 2000 μg mL^{-1} and IC_{50} > 512 μg mL^{-1}), which led to the highest selectivity of bacteria over host cells (TI of 21), and were the most promising polymers in our collection.

4. Conclusion

In this study, we evaluated the effect of different hydrophilic monomers on the biocompatibility and antibacterial activity of antimicrobial polymers. The results revealed that, unlike the hydrophobic group, the hydrophilic group did not disrupt the bacteria membrane. They did, however, have an indirect influence on bioactivity through tuning the hydrophobic/hydrophilic balance and the global hydrophobicity, leading to a change in the aqueous characteristics of the polymers. Therefore, in antimicrobial polymer design, an appropriate hydrophobic/hydrophilic balance and the structural features of the hydrophilic group, such as length, flexibility, and hydrophilicity of the hydrophilic chain are key factors for optimising biocompatibility toward the host biocomponents without interfering with their antimicrobial potency. In our collection, the antimicrobial polymers with the highest selectively for bacterial cells over mammalian cells were those containing PEG.

Conflicts of interest

There are no conflicts to declare.

Acknowledgements

This work was supported by the Australian Research Council (DP190100067, C. B.). PP acknowledges the receipt of an Australian Government Research Training Program (RTP) Scholarship. We also acknowledge the facilities and technical assistance provided by the Mark Wainwright Analytical Centre at UNSW Australia *via* the Nuclear Magnetic Resonance Facility; Joanna Biazik-Richmond and Gregory Harm of the Cell Culture Facility within the MWAC for their introduction to and support with the cell culture work.

References

1 D. M. Brogan and E. Mossialos, *Glob. Health*, 2016, **12**, 8.
2 S. J. Lam, N. M. O'Brien-Simpson, N. Pantarat, A. Sulistio, E. H. H. Wong, Y.-Y. Chen, J. C. Lenzo, J. A. Holden, A. Blencowe, E. C. Reynolds and G. G. Qiao, *Nat. Microbiol.*, 2016, **1**, 16162.
3 A. Pop-Vicas, J. Strom, K. Stanley and E. M. C. D'Agata, *Clin. J. Am. Soc. Nephrol.*, 2008, **3**, 752–758.
4 K. Lewis, *Nat. Rev. Drug Discovery*, 2013, **12**, 371–387.
5 N. Mookherjee, M. A. Anderson, H. P. Haagsman and D. J. Davidson, *Nat. Rev. Drug Discovery*, 2020, **19**, 311–332.
6 J. Tan, J. Tay, J. Hedrick and Y. Y. Yang, *Biomaterials*, 2020, **252**, 120078.
7 M. Zasloff, *Nature*, 2002, **415**, 389–395.
8 H. Takahashi, G. A. Caputo and K. Kuroda, *Biomater. Sci.*, 2021, **9**, 2758–2767.
9 R. E. W. Hancock and H.-G. Sahl, *Nat. Biotechnol.*, 2006, **24**, 1551–1557.
10 A. G. Elliott, J. X. Huang, S. Neve, J. Zuegg, I. A. Edwards, A. K. Cain, C. J. Boinett, L. Barquist, C. V. Lundberg, J. Steen, M. S. Butler, M. Mobli, K. M. Porter, M. A. T. Blaskovich, S. Lociuro, M. Strandh and M. A. Cooper, *Nat. Commun.*, 2020, **11**, 3184.
11 H. Takahashi, G. A. Caputo, S. Vemparala and K. Kuroda, *Bioconjugate Chem.*, 2017, **28**, 1340–1350.
12 E. F. Palermo and K. Kuroda, *Appl. Microbiol. Biotechnol.*, 2010, **87**, 1605–1615.
13 S. Perrier, *Macromolecules*, 2017, **50**, 7433–7447.
14 N. Corrigan, K. Jung, G. Moad, C. J. Hawker, K. Matyjaszewski and C. Boyer, *Prog. Polym. Sci.*, 2020, **111**, 101311.
15 C. J. Hawker, A. W. Bosman and E. Harth, *Chem. Rev.*, 2001, **101**, 3661–3688.
16 A. Anastasaki, V. Nikolaou, G. Nurumbetov, P. Wilson, K. Kempe, J. F. Quinn, T. P. Davis, M. R. Whittaker and D. M. Haddleton, *Chem. Rev.*, 2016, **116**, 835–877.
17 S. J. Lam, E. H. H. Wong, C. Boyer and G. G. Qiao, *Prog. Polym. Sci.*, 2018, **76**, 40–64.
18 A. C. G. Weiss, S. J. Shirbin, H. G. Kelly, Q. A. Besford, S. J. Kent and G. G. Qiao, *ACS Appl. Mater. Interfaces*, 2021, **13**, 33821–33829.
19 S.-J. Richards, A. Jones, R. M. F. Tomás and M. I. Gibson, *Chem. – Eur. J.*, 2018, **24**, 13758–13761.
20 C. Stubbs, T. Congdon, J. Davis, D. Lester, S.-J. Richards and M. I. Gibson, *Macromolecules*, 2019, **52**, 7603–7612.
21 A. Kuroki, P. Sangwan, Y. Qu, R. Peltier, C. Sanchez-Cano, J. Moat, C. G. Dowson, E. G. L. Williams, K. E. S. Locock, M. Hartlieb and S. Perrier, *ACS Appl. Mater. Interfaces*, 2017, **9**, 40117–40126.
22 P. Gurnani, T. Floyd, J. Tanaka, C. Stubbs, D. Lester, C. Sanchez-Cano and S. Perrier, *Polym. Chem.*, 2020, **11**, 1230–1236.
23 B. P. Mowery, A. H. Lindner, B. Weisblum, S. S. Stahl and S. H. Gellman, *J. Am. Chem. Soc.*, 2009, **131**, 9735–9745.
24 Y. Yang, Z. Cai, Z. Huang, X. Tang and X. Zhang, *Polym. J.*, 2018, **50**, 33–44.
25 E. F. Palermo, I. Sovadinova and K. Kuroda, *Biomacromolecules*, 2009, **10**, 3098–3107.
26 E. F. Palermo, S. Vemparala and K. Kuroda, *Biomacromolecules*, 2012, **13**, 1632–1641.
27 K. Kuroda, G. A. Caputo and W. F. DeGrado, *Chem. – Eur. J.*, 2009, **15**, 1123–1133.
28 P. T. Phuong, S. Oliver, J. He, E. H. H. Wong, R. T. Mathers and C. Boyer, *Biomacromolecules*, 2020, **21**, 5241–5255.
29 E. F. Palermo, K. Lienkamp, E. R. Gillies and P. J. Ragogna, *Angew. Chem.*, 2019, **131**, 3728–3731.
30 P. R. Judzewitsch, L. Zhao, E. H. H. Wong and C. Boyer, *Macromolecules*, 2019, **52**, 3975–3986.
31 E. F. Palermo and K. Kuroda, *Biomacromolecules*, 2009, **10**, 1416–1428.
32 B. Hisey, P. J. Ragogna and E. R. Gillies, *Biomacromolecules*, 2017, **18**, 914–923.
33 M. Hirayama, *Biocontrol Sci.*, 2011, **16**, 23–31.

34 Y. Hu, J. Zhao, J. Zhang, Z. Zhu and J. Rao, *ACS Macro Lett.*, 2021, **10**, 990–995.
35 B. Zhang, M. Li, M. Lin, X. Yang and J. Sun, *Biomater. Sci.*, 2020, **8**, 6969–6977.
36 T. J. Cuthbert, B. Hisey, T. D. Harrison, J. F. Trant, E. R. Gillies and P. J. Ragogna, *Angew. Chem., Int. Ed.*, 2018, **57**, 12707–12710.
37 T.-K. Nguyen, S. J. Lam, K. K. K. Ho, N. Kumar, G. G. Qiao, S. Egan, C. Boyer and E. H. H. Wong, *ACS Infect. Dis.*, 2017, **3**, 237–248.
38 B. C. Allison, B. M. Applegate and J. P. Youngblood, *Biomacromolecules*, 2007, **8**, 2995–2999.
39 P. H. Sellenet, B. Allison, B. M. Applegate and J. P. Youngblood, *Biomacromolecules*, 2007, **8**, 19–23.
40 P. R. Judzewitsch, T.-K. Nguyen, S. Shanmugam, E. H. H. Wong and C. Boyer, *Angew. Chem., Int. Ed.*, 2018, **57**, 4559–4564.
41 C. a. L. S. I. (CLSI), *Methods for Dilution Antimicrobial Susceptibility Tests for Bacteria That Grow Aerobically; Approved Standard*, 9th edn, 2012.
42 D. Dutta, A. K. Vijay, N. Kumar and M. D. P. Willcox, *Invest. Ophthalmol. Visual Sci.*, 2016, **57**, 5616–5624.
43 D. Dutta, N. Cole, N. Kumar and M. D. P. Willcox, *Invest. Ophthalmol. Visual Sci.*, 2013, **54**, 175–182.
44 K. Parkatzidis, N. P. Truong, M. N. Antonopoulou, R. Whitfield, D. Konkolewicz and A. Anastasaki, *Polym. Chem.*, 2020, **11**, 4968–4972.
45 S. Shanmugam, J. Xu and C. Boyer, *J. Am. Chem. Soc.*, 2015, **137**, 9174–9185.
46 G. Ng, J. Yeow, R. Chapman, N. Isahak, E. Wolvetang, J. J. Cooper-White and C. Boyer, *Macromolecules*, 2018, **51**, 7600–7607.
47 C. A. Figg, J. D. Hickman, G. M. Scheutz, S. Shanmugam, R. N. Carmean, B. S. Tucker, C. Boyer and B. S. Sumerlin, *Macromolecules*, 2018, **51**, 1370–1376.
48 S. E. Seo, E. H. Discekici, Y. Zhang, C. M. Bates and C. J. Hawker, *J. Polym. Sci.*, 2020, **58**, 70–76.
49 J. Niu, D. J. Lunn, A. Pusuluri, J. I. Yoo, M. A. O'Malley, S. Mitragotri, H. T. Soh and C. J. Hawker, *Nat. Chem.*, 2017, **9**, 537–545.
50 R. Namivandi-Zangeneh, Y. Yang, S. Xu, E. H. H. Wong and C. Boyer, *Biomacromolecules*, 2020, **21**, 262–272.
51 A. Gessner, R. Waicz, A. Lieske, B. R. Paulke, K. Mäder and R. H. Müller, *Int. J. Pharm.*, 2000, **196**, 245–249.
52 M. Malmsten, *Colloids Surf., B*, 1995, **3**, 297–308.
53 Q. Dai, Y. Yan, J. Guo, M. Björnmalm, J. Cui, H. Sun and F. Caruso, *ACS Macro Lett.*, 2015, **4**, 1259–1263.
54 Z. Pang, R. Raudonis, B. R. Glick, T.-J. Lin and Z. Cheng, *Biotechnol. Adv.*, 2019, **37**, 177–192.
55 E. B. M. Breidenstein, C. de la Fuente-Núñez and R. E. W. Hancock, *Trends Microbiol.*, 2011, **19**, 419–426.
56 J. A. Baird, R. Olayo-Valles, C. Rinaldi and L. S. Taylor, *J. Pharm. Sci.*, 2010, **99**, 154–168.
57 J. T. Huckaby, T. M. Jacobs, Z. Li, R. J. Perna, A. Wang, N. I. Nicely and S. K. Lai, *Commun. Chem.*, 2020, **3**, 124.
58 S. N. Rampersad, *Sensors*, 2012, **12**, 12347–12360.
59 S. Oliver, E. Yee, M. Kavallaris, O. Vittorio and C. Boyer, *Macromol. Biosci.*, 2018, 1700239.
60 S. Oliver, D. S. Thomas, M. Kavallaris, O. Vittorio and C. Boyer, *Polym. Chem.*, 2016, **7**, 2542–2552.
61 S. L. Voytik-Harbin, A. O. Brightman, B. Waisner, C. H. Lamar and S. F. Badylak, *In Vitro Cell. Dev. Biol.: Anim.*, 1998, **34**, 239–246.
62 S. Aykul and E. Martinez-Hackert, *Anal. Biochem.*, 2016, **508**, 97–103.
63 S. Schaefer, T. T. P. Pham, S. Brunke, B. Hube, K. Jung, M. D. Lenardon and C. Boyer, *ACS Appl. Mater. Interfaces*, 2021, **13**(23), 27430–27444.
64 B. Lindman and P. Alexandridis, in *Amphiphilic Block Copolymers*, ed. P. Alexandridis and B. Lindman, Elsevier Science B.V., Amsterdam, 2000, pp. 1–12. DOI: 10.1016/B978-044482441-7/50002-5.
65 H. J. Dyson, P. E. Wright and H. A. Scheraga, *Proc. Natl. Acad. Sci. U. S. A.*, 2006, **103**, 13057–13061.
66 G. Rani, K. Kuroda and S. Vemparala, *Soft Matter*, 2021, **17**, 2090–2103.
67 G. Rani, K. Kuroda and S. Vemparala, *J. Phys.: Condens. Matter*, 2020, **33**, 064003.
68 M. A. Rahman, M. Bam, E. Luat, M. S. Jui, M. S. Ganewatta, T. Shokfai, M. Nagarkatti, A. W. Decho and C. Tang, *Nat. Commun.*, 2018, **9**, 5231.
69 D. J. Paterson, M. Tassieri, J. Reboud, R. Wilson and J. M. Cooper, *Proc. Natl. Acad. Sci. U. S. A.*, 2017, **114**, E8324.
70 M. Tanaka, T. Hayashi and S. Morita, *Polym. J.*, 2013, **45**, 701–710.
71 M. Tanaka, K. Sato, E. Kitakami, S. Kobayashi, T. Hoshiba and K. Fukushima, *Polym. J.*, 2015, **47**, 114–121.
72 J. M. Harris and R. B. Chess, *Nat. Rev. Drug Discovery*, 2003, **2**, 214–221.
73 K. Knop, R. Hoogenboom, D. Fischer and U. S. Schubert, *Angew. Chem., Int. Ed.*, 2010, **49**, 6288–6308.
74 H. Kitano, K. Ichikawa, M. Ide, M. Fukuda and W. Mizuno, *Langmuir*, 2001, **17**, 1889–1895.
75 V. P. Torchilin and M. I. Papisov, *J. Liposome Res.*, 1994, **4**, 725–739.
76 J. Zheng, L. Li, S. Chen and S. Jiang, *Langmuir*, 2004, **20**, 8931–8938.